Cell Host & Microbe
Article

A Hydrolase of Trehalose Dimycolate Induces Nutrient Influx and Stress Sensitivity to Balance Intracellular Growth of *Mycobacterium tuberculosis*

Yong Yang,[1] Kathleen Kulka,[1] Ronald C. Montelaro,[1,2,3] Todd A. Reinhart,[1] James Sissons,[4] Alan Aderem,[4] and Anil K. Ojha[1,*]
[1]Department of Infectious Diseases and Microbiology
[2]Department of Microbiology and Molecular Genetics
[3]Center for Vaccine Research
University of Pittsburgh, Pittsburgh, PA 15261, USA
[4]Seattle Biomedical Research Institute, 307 Westlake Avenue North, Seattle, WA 98109, USA
*Correspondence: ano7@pitt.edu
http://dx.doi.org/10.1016/j.chom.2014.01.008

SUMMARY

Chronic tuberculosis in an immunocompetent host is a consequence of the delicately balanced growth of *Mycobacterium tuberculosis* (Mtb) in the face of host defense mechanisms. We identify an Mtb enzyme ($Tdmh_{Mtb}$) that hydrolyzes the mycobacterial glycolipid trehalose dimycolate and plays a critical role in balancing the intracellular growth of the pathogen. $Tdmh_{Mtb}$ is induced under nutrient-limiting conditions and remodels the Mtb envelope to increase nutrient influx but concomitantly sensitizes Mtb to stresses encountered in the host. Consistent with this, a $\Delta tdmh_{Mtb}$ mutant is more resilient to stress and grows to levels higher than those of wild-type in immunocompetent mice. By contrast, mutant growth is retarded in $MyD88^{-/-}$ mice, indicating that $Tdmh_{Mtb}$ provides a growth advantage to intracellular Mtb in an immunocompromised host. Thus, the effects and countereffects of $Tdmh_{Mtb}$ play an important role in balancing intracellular growth of Mtb in a manner that is directly responsive to host innate immunity.

INTRODUCTION

The global burden of tuberculosis (TB), which kills over a million people every year, is perpetuated by the vast majority of chronic and often asymptomatic infections with *Mycobacterium tuberculosis* (Mtb), estimated to be prevalent in about one-third of the world's population (WHO, 2012). Chronic infection with Mtb in an immunocompetent host is associated with controlled but persisting bacterial burden, established after an early phase of relatively rapid growth against the host-imposed antimicrobial activities (Cooper et al., 2011; Ernst, 2012; Lin et al., 2009; Stallings and Glickman, 2010). Furthermore, long-term infections of Mtb, even without clinical symptoms, are likely associated with a dynamic host-pathogen interaction. This is supported by evidence for active bacterial replication (Ford et al., 2011; Gill et al., 2009), continuous engagement of host immune system (Ulrichs et al., 2005), and the presence of drug-responsive lesions (Park et al., 2008) in chronic or latent TB. A question then arises as to what molecular mechanisms balance the interaction such that both the pathogen's growth and the host inflammatory response are contained below a symptomatic threshold in an immunocompetent host. From the host perspective, a tightly regulated process of granuloma formation, involving optimum secretion of proinflammatory cytokines followed by recruitment of immune cells at the infection sites, has been implicated in containing the infection (Chan and Flynn, 2004; Ernst, 2012; Tobin et al., 2012; Yang et al., 2012). It is further emerging that an optimum inflammatory response in macrophages that is high enough to trigger effective antibacterial activity, yet below the threshold of cellular necroptosis, is most effective in restricting mycobacterial growth, implying that Mtb growth is most likely restricted in the intracellular environment (Roca and Ramakrishnan, 2013). Among the key antimicrobial intracellular factors are free radicals, low pH, antimicrobial peptides, and digestive enzymes (Beutler, 2004).

From the pathogen's perspective, long-term survival would involve successful adaptation to limiting nutrients in the intracellular environment while simultaneously resisting host-imposed antimicrobial activities. Nutrient acquisition and stress resistance are mechanistically distinct processes in bacteria. However, it is extremely likely that these pathways intersect at the cell envelope, which constitutes an entry point for nutrients as well as antimicrobials in the environment. The mycobacterial envelope is stratified into a cytoplasmic membrane of phospholipids, a core cell wall of mycolyl-arabinogalactan-peptidoglycan (mAGP) complex, and a membrane-like outer layer called mycomembrane (MoM) (Brennan and Nikaido, 1995; Niederweis et al., 2010). This architecture is broadly similar to the Gram-negative bacterial envelope, in which the lipid bilayers of inner and outer membranes are the two primary permeability barriers against environmental solutes (Nikaido, 2003). While solute-specific transporters facilitate the import of hydrophilic nutrients across the inner membrane, entry across the outer membrane is facilitated either by passive diffusion across the lipid matrix or through the channel proteins, called porins (Niederweis, 2008; Nikaido, 2003). The charged amino acids lining the water-filled channels of porins facilitate the entry of a broad spectrum of

hydrophilic substrates from the environment (Nikaido, 2003). Four porins (MspA–MspD) have been identified in the nonpathogenic mycobacterial species, *Mycobacterium smegmatis* (Stephan et al., 2005). Deletion of the primary porin, MspA, retards the influx of hydrophilic nutrients from the environment, and its overexpression in Mtb and *M. bovis* (BCG) increases nutrient influx (Mailaender et al., 2004; Stephan et al., 2005). However, induction of porin-dependent outer membrane permeability also increases sensitivity to a variety of chemical stresses and retards the intracellular growth of Mtb in cultured macrophages (Fabrino et al., 2009; Mailaender et al., 2004; Purdy et al., 2009). Taken together, these studies suggest that if intracellular Mtb were to adapt in a healthy host by inducing permeability of MoM for efficient nutrient uptake, the concomitant exposure to stress factors could self-limit its growth. Although porin-like proteins and associated nonselective permeability of MoM are likely to be present in Mtb (Molle et al., 2006; Siroy et al., 2008), the mechanism underlying the regulation of envelope permeability in intracellular Mtb remains unclear.

The lipid bilayer of MoM is considered to be made of mycolic acids of mAGP as the inner leaflet and noncovalently associated glycolipids and phospholipids as the outer leaflet (Hoffmann et al., 2008; Niederweis et al., 2010). Among the noncovalently associated glycolipids, the mycolyl esters of trehalose—trehalose monomycolates (TMMs) and trehalose dimycolates (TDMs)—are the predominant species (Takayama et al., 2005). TMM is the common donor of mycolyl chain in the synthesis of mAGP and TDM (Belisle et al., 1997; Takayama et al., 2005). TDM has long been studied as a cord factor, conferring a cord-like appearance to Mtb in vitro, with strong immunomodulatory activities (Hunter et al., 2006; Ishikawa et al., 2009; Rao et al., 2006). However, recent studies suggest that TDM could be a structural component of MoM (Ojha et al., 2010; Yang et al., 2013). An uncontrolled exogenous exposure of mycobacteria to a serine hydrolase of TDM from *M. smegmatis*, called $Tdmh_{Ms}$, leads to a rapid depletion of trehalose mycolates and subsequent rupturing of the envelope (Ojha et al., 2010; Yang et al., 2013). Interestingly, one of the products of TDM hydrolysis, free mycolic acid (FM), is an abundant extracellular component of in vitro biofilms of both Mtb and *M. smegmatis*, although the physiological role of $Tdmh_{Ms}$ during mycobacterial growth in biofilms is unclear (Ojha et al., 2008; Ojha et al., 2010).

Because a TDM hydrolyzing activity in Mtb lysates was also detected during the discovery of $Tdmh_{Ms}$ (Ojha et al., 2010), we sought to identify the enzyme in Mtb and investigate its impact on TB pathogenesis. In this study, we show that Rv3451 is the primary TDM hydrolase in Mtb and is induced under limiting nutrients. Its activity facilitates nutrient influx but also substantially sensitizes the pathogen to the stresses prevalent in the host. Further, we provide evidence that the effects and countereffects of $Tdmh_{Mtb}$ play an important role in balancing intracellular growth of Mtb in a manner that is directly responsive to host innate immunity.

RESULTS

Identification of TDM Hydrolases in Mtb

Two tandemly organized serine esterases in the Mtb genome, Rv3451 and Rv3452, have over 50% similarity to $tdmh_{Ms}$ (Figure 1A). Importantly, both contain the conserved catalytic triad of Ser (in GXSXG motif), Asp, and His (Figure 1A). We therefore addressed whether these two open reading frames (ORFs) encode TDM hydrolases. Figures 1B and S1 (available online) show the release of ^{14}C-labeled FM when lysates of recombinant *M. smegmatis* lacking $Tdmh_{Ms}$ (Ojha et al., 2010) and expressing either Rv3451 (mc^2155:*Δtdmh*$_{Ms}$*:pRv3451*) or Rv3452 (mc^2155:*Δtdmh*$_{Ms}$*:pRv3452*) were mixed with purified ^{14}C-labeled TDM (Figures 1B and S1). The activity of Rv3452 lysate, however, was weaker than Rv3451 (Figure 1B). Moreover, five other putative cutinase-like esterases of Mtb did not produce such activity (Figure 1C). Therefore, we designate Rv3451 as $tdmh_{Mtb}$, and Rv3452 as $tdmh_{Mtb2}$. In addition, we also noted that the activity in mc^2155:*Δtdmh*$_{Ms}$*:pRv3451* lysate was excluded from the cytosolic fraction (Figure 1D), suggesting that $Tdmh_{Mtb}$ is exported to the envelope.

The presence of TDM hydrolases in Mtb indicates that this glycolipid is turned over into FM under certain unknown physiological conditions. Because FM is highly abundant in the 4-week biofilms of Mtb (Ojha et al., 2008), we examined TDM turnover under these conditions. An isogenic *Δtdmh*$_{Mtb}$ mutant of an attenuated Mtb strain, mc^27000 (Ojha et al., 2008), accumulated ~3-fold more TDM than the parent wild-type in 4-week biofilms (Figures 2A–2D), suggesting a slower turnover of the glycolipid in the biofilms, although the appearance of the mutant biofilms was indistinguishable from that of the wild-type. Moreover, the hydrolase-dependent TDM turnover appeared to be specifically induced in the later growth phase, since TDM levels in the mutant were similar to those of wild-type at the 2-week stage (Figure 2D). Furthermore, we did not notice any other significant change in the lipids in 4-week biofilms of *Δtdmh*$_{Mtb}$ (Figure S2). TDM therefore is likely among the primary substrates of the esterase, although TDM hydrolysis only partly contributes to the FM pool since its level is reduced by only about 20% in *Δtdmh*$_{Mtb}$ (data not shown). Thus, FM accumulation likely occurs through additional unknown mechanisms.

$Tdmh_{Mtb}$ Increases Nutrient Influx under Limiting Conditions but Sensitizes Mtb to Stresses

We next addressed the physiological significance of $Tdmh_{Mtb}$. An earlier microarray study observed induced transcription of $Tdmh_{Mtb}$ after 96 hr nutritional downshift of Mtb cultures in vitro (Betts et al., 2002). We confirmed a similar increase in mRNA abundance of $Tdmh_{Mtb}$ upon 96 hr exposure of normal planktonic mc^27000 to a nutrient-limiting media (7H9 base without supplements) and in 4-week biofilms (Figure S3A). This raises a possibility that $Tdmh_{Mtb}$-dependent envelope remodeling could facilitate appropriate adaptative response to nutrient limitation. To investigate this further, we first analyzed changes in nutrient influx upon exposure of wild-type Mtb to limiting conditions. Interestingly, 96 hr incubation in 7H9 base medium increases glycerol influx in bacilli by ~40%, although prolonged incubation (6 weeks) led to a decrease by ~4-fold (Figure 3A). We further noted that under these conditions Mtb maintained slow but distinctively positive growth for about 2 weeks, and regenerated in fresh nutrients like a normal nutrient-rich culture, before assuming stationary phase (Figures 3B and S3B). These data demonstrate a two-stage adaptation to limiting nutrients in

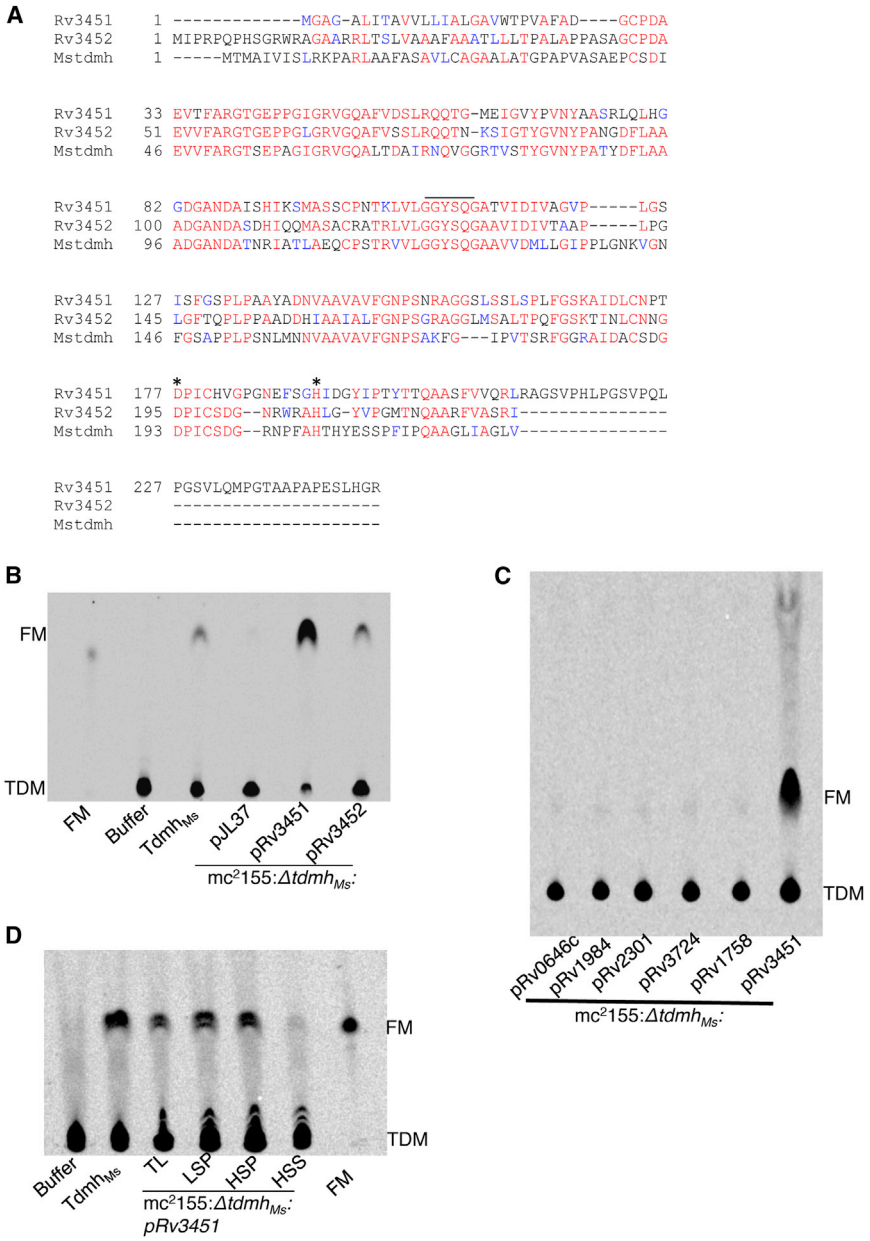

Figure 1. Rv3451 and Rv3452 Are TDM Hydrolases in Mtb

(A) Alignment of Rv3451 and Rv3452 protein sequences with $Tdmh_{Ms}$, originally marked as Mstdmh (Ojha et al., 2010). The catalytic triad of Ser, Asp, and His are indicated.

(B) Radio-thin-layer chromatography (radio-TLC) analysis of lipids in a mixture containing ^{14}C TDM and lysates from recombinant *M. smegmatis*, mc^2155:$\Delta tdmh_{Ms}$, transformed with either empty plasmid (pJL37), pRv3451, or pRv3452 (see also Figure S1). Reactions with purified $Tdmh_{Ms}$ and storage buffer were positive and negative controls, respectively. Purified FM was the marker.

(C) Absence of TDM hydrolyzing activity in the lysates of mc^2155:$\Delta tdmh_{Ms}$ expressing five other hydrolases (Rv0646c, Rv1984, Rv2301, Rv3724, and Rv1758). These hydrolases were cloned on the same plasmid backbone (pJL37), under constitutive hsp60 promoter, as that used for Rv3451. These plasmids are indicated below each lane. mc^2155:$\Delta tdmh_{Ms}$:*pRv3451* is the positive control.

(D) The hydrolase activity of $Tdmh_{Mtb}$ (Rv3451) in cellular factions of mc^2155:$\Delta tdmh_{Ms}$:*pRv3451*. TL, total lysate; LSP, low-speed pellet (obtained from centrifugation of TL at 20,000 × *g* for 60 min); HSP, high-speed pellet (obtained from centrifugation of low-speed supernatant at 100,000 × *g* for 60 min); HSS, high-speed supernatant (obtained from the same centrifugation as that described for HSP). Purified FM was loaded as the marker. See also Figure S1.

Mtb: an early response that involves growth maintenance under moderate limitation of nutrients by inducing the influx, followed by a late response of slow nutrient influx and metabolic slowdown under extreme limitation. We next investigated whether $Tdmh_{Mtb}$ has any role in maintaining Mtb growth under limiting nutrients. This was preliminarily suggested by an increase in the influx of nutrients upon constitutive expression of $tdmh_{Mtb}$ in *M. smegmatis* through the *hsp60* promoter (Figure 3C). We further observed that the influx of acetate, phosphate, and glycerol was retarded in $\Delta tdmh_{Mtb}$, relative to the wild-type, when the cultures were preexposed to limiting nutrients for 96 hr (Figure 3D). The mutant had no such defect in a normal culture (Figure S3C). Interestingly, complementation of $\Delta tdmh_{Mtb}$ required a genomic fragment containing both $tdmh_{Mtb}$ and $tdmh_{Mtb2}$ (Figure 3D). It is notable that $tdmh_{Mtb2}$ transcripts were reduced by 50% in $\Delta tdmh_{Mtb}$, but restoration of expression of either $tdmh_{Mtb}$ or $tdmh_{Mtb2}$ alone was insufficient for complementing the mutant (Figures 3D, S3D, and S3E). The complementation analysis not only shows that $tdmh_{Mtb2}$ is transcriptionally linked to $tdmh_{Mtb}$, but also suggests that the two hydrolases likely interact with each other. Reduced influx of nutrients in $\Delta tdmh_{Mtb}$ was further consistent with its retarded growth in media with limiting glycerol (Figure 3E). The data together suggest that TDM hydrolases could comprise components of an adaptative response in Mtb to facilitate its growth under nutrient-limiting conditions by inducing the nonselective permeability of the envelope, thereby increasing influx of multiple nutrients.

Ectopically induced nonselective permeability of the envelope by recombinant porins also increases sensitivity of Mtb to a wide range of environmental stresses (Fabrino et al., 2009; Mailaender et al., 2004; Purdy et al., 2009). We therefore reasoned that $Tdmh_{Mtb}$-dependent envelope remodeling under limiting nutrients, or in biofilms, could concomitantly sensitize bacteria to a variety of stresses. Indeed, biofilms of the mutant were significantly more tolerant than the wild-type to peroxide and lysozyme, the predominant antimicrobial agents of the mammalian innate immune system (Beutler, 2004) (Figure 3F).

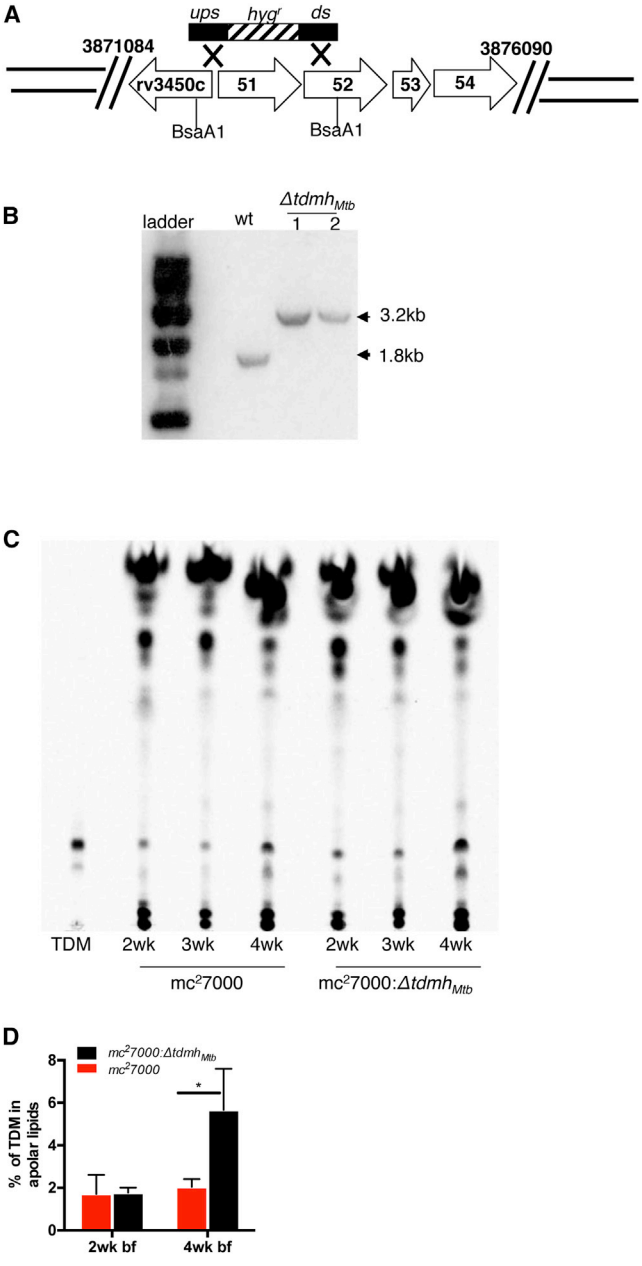

Figure 2. Accumulation of TDM in mc^{2}7000:*Δtdmh$_{Mtb}$*

(A) Schematic representation of genomic organization of *rv3451* (*tdmh$_{Mtb}$*) and *rv3452* (*tdmh$_{Mtb2}$*), and the allelic exchange substrate including upstream (*ups*) and downstream (*ds*) regions used for replacement of *tdmh$_{Mtb}$* with *hyg^r*.

(B) Southern blot of BsaAI-digested genomic DNA from the parent wild-type (mc^{2}7000) and two *hyg^r* colonies (*Δtdmh$_{Mtb}$*) probed with *ups*. Data in represent mean ± SE (n = 3).

(C) A representative radio-TLC of apolar lipids extractable from Mtb strains, mc^{2}7000, and mc^{2}7000:*Δtdmh$_{Mtb}$* at 2-, 3-, and 4-week stages of biofilms. Purified TDM is the marker.

(D) Quantitative analysis of the level of TDM as a percentage of total apolar lipids in mc^{2}7000 (wild-type) and mc^{2}7000:*Δtdmh$_{Mtb}$* (mutant) in 2- and 4-week stages of biofilms (see also Figure S2 for the complete lipid profile). Data represent mean ± SE (n = 3). *p < 0.05 (t test).

Ectopic Induction of Tdmh$_{Ms}$ Increases Nutrient Influx and Stress Sensitivity

Despite several attempts, we could neither detect the physiological levels of Tdmh$_{Mtb}$ proteins in Mtb nor obtain its purified active form using recombinant systems. Therefore, to affirm the correlation between TDM hydrolase activity and the phenotypes of *Δtdmh$_{Mtb}$*, we investigated the effect of ectopic expression of a well-characterized heterologous Tdmh, Tdmh$_{Ms}$, in a nutrient-rich culture of Mtb. Interestingly, despite the deleterious consequence of exogenous exposure to Tdmh$_{Ms}$ (Yang et al., 2013), its stable expression from a plasmid-borne acetamide-inducible promoter could be achieved in Mtb without any apparent impact on the growth (Figures 4A and 4B). The in vivo activity of the enzyme is therefore likely controlled by an unknown posttranslational mechanism. Induced expression of Tdmh$_{Ms}$ in nutrient-rich culture led to a significant increase in the influx of glycerol, acetate, and phosphate (Figure 4C). Moreover, induced expression of Tdmh$_{Ms}$ also increased bacterial sensitivity to peroxide, lysozyme, and LL37, a cathelicidin-related antimicrobial peptide (Figure 4D). Furthermore, induction of Tdmh$_{Ms}$ in Mtb(Erd) accelerated its growth in media with limiting glycerol (Figure 4E). We therefore conclude that activity of TDM hydrolase produces structural changes in the envelope that increase its permeability to nutrients but also expose the bacilli to environmental hazards.

TDM Hydrolases Self-Restrict Intracellular Growth of Mtb in Immunocompetent Hosts

Rv3451(*tdmh$_{Mtb}$*) is among the 215 core genes induced within the first 24 hr of Mtb infection in macrophages, and the upregulated expression continues during prolonged existence of the pathogen in the host cells (Rohde et al., 2012). Moreover, Tdmh$_{Mtb2}$ antibodies have been detected in the sera of TB patients (Brust et al., 2011). These suggest that Mtb utilizes the activity of TDM hydrolases in vivo. The induced expression of *tdmh$_{Mtb}$* in macrophages further suggests that the hydrolase activity could be utilized by the pathogen to increase nutrient influx in limiting intracellular conditions. We tested this idea by adding ^{14}C-labeled acetate into media of macrophages infected with either *Δtdmh$_{Mtb}$*, its respective wild-type, or the complement strain, and comparing the radioactivity accumulated in the intracellular bacilli. This approach was facilitated through efficient separation of Mtb from lysates of infected macrophages with TB-Beads. TB-Beads are commercially available paramagnetic microparticles (<5 μm) that bind to Mtb bacilli with very high affinity and specificity (Wilson et al., 2010). Over 90% of the bacteria from macrophage lysates could be captured on TB-Beads (Figure S4A). Furthermore, nonspecific binding was very low, yielding a quantitative estimation of radioactivity specifically associated with intracellular Mtb (Figure S4B). Indeed, *Δtdmh$_{Mtb}$* accumulated 50% less radioactivity than the other strains, suggesting that the hydrolases facilitate nutrient influx in Mtb in vivo (Figure 5A). Surprisingly, *Δtdmh$_{Mtb}$* was more robust than wild-type, Mtb(Erd), and the complemented strains in preactivated primary bone marrow-derived macrophages (BMMs) from immunocompetent mice, C57BL/6 (Figures 5B and S4C), suggesting that the hydrolase-dependent sensitization to stresses could perhaps play a dominant role in determining the overall survival of Mtb in immunocompetent

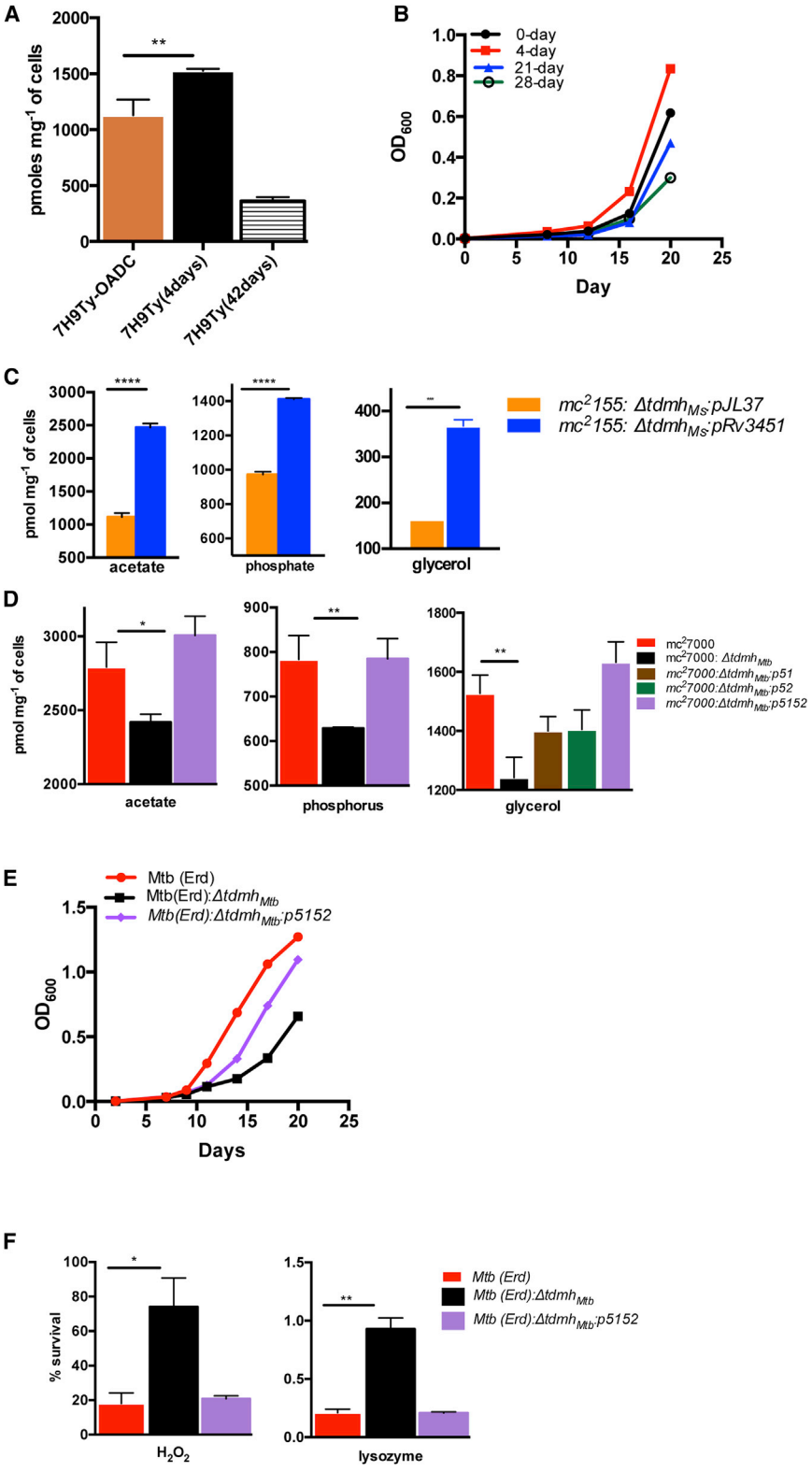

Figure 3. Correlation between Induced Tdmh$_{Mtb}$ Activity and Increased Nonselective Permeability of the Mycobacterial Envelope under Limiting Nutrients

(A) Influx of glycerol over 2 hr in mc^{2}7000 incubated in normal (7H9TyOADC) and nutrient-limiting media (7H9Ty) for the indicated time. Ty denotes 0.05% v/v tyloxapol.

(B) Regeneration of Mtb(Erd) in 7H9Ty with 0.1% v/v glycerol from a culture maintained in 7H9Ty for the indicated time.

(C) Accumulation of acetate, phosphorus, and glycerol over 30 min by mc^{2}155:*Δtdmh$_{Ms}$* transformed with either pJL37 or pRv3451.

(D) Accumulation of acetate, phosphorus, and glycerol over 2 hr by cultures of mc^{2}7000, mc^{2}7000:*Δtdmh$_{Mtb}$*, and mc^{2}7000:*Δtdmh$_{Mtb}$* expressing Rv3451 (mc^{2}7000:*Δtdmh$_{Mtb}$:p51*), Rv3452 (mc^{2}7000:*Δtdmh$_{Mtb}$:p52*), or Rv3451-52 (mc^{2}7000:*Δtdmh$_{Mtb}$:p5152*) in nutrient-limiting media (see also Figure S3).

(E) Growth of Mtb(Erd), *Δtdmh$_{Mtb}$* mutant, and the complement strain (mc^{2}7000:*Δtdmh$_{Mtb}$:p5152*) in 7H9Ty with 0.1% v/v glycerol.

(F) Sensitivity of 4-week biofilms of Mtb (Erd), Mtb (Erd):*Δtdmh$_{Mtb}$*, and Mtb (Erd):*Δtdmh$_{Mtb}$:p5152* to H_2O_2 (40 mM) and lysozyme (6 μg/ml). See also Figure S3.

Data in (A), (C), (D), and (F) represent mean ± SE (n = 3). *p < 0.05, **p < 0.01, ****p < 0.0001 (t test).

macrophages. We therefore evaluated the intracellular fitness of Mtb(Erd), *Δtdmh$_{Mtb}$*, and the complemented strain in a stress test, which involved direct measurement of their sensitivity to isoniazid. Figure 5C shows that intracellular *Δtdmh$_{Mtb}$* indeed survives significantly better than the wild-type and complemented strains under isoniazid stress (Figure 5C). Interestingly, primary BMMs infected with *Δtdmh$_{Mtb}$* produced proinflammatory cytokine, tumor necrosis factor alpha (TNF-α), at a level lower than those produced by BMMs infected with wild-type or the complemented strains (Figure S4D). This suggests a suboptimal activation of the mutant-infected BMM, although underlying mechanisms remain unknown.

An improved survival of *Δtdmh$_{Mtb}$* mutant in the macrophages was further supported by its better growth during the early phase of infection in immunocompetent C57BL/6 mice. During the first 3 weeks of infection, the mutant produced a burden in the lungs about 4-fold higher than those produced by parent wild-type and complemented strains (Figure 5D). Interestingly, severe splenomegaly and lung pathology, with greater alveolar, peribronchiolar, and perivascular infiltrations, as well as congestion in the conducting airways were observed during chronic phase of *Δtdmh$_{Mtb}$* infection (Figures S4E and S4F), although the basis of severe pathology remains unclear. Consistent with the severe pathology, however, mice infected with *Δtdmh$_{Mtb}$* had shorter

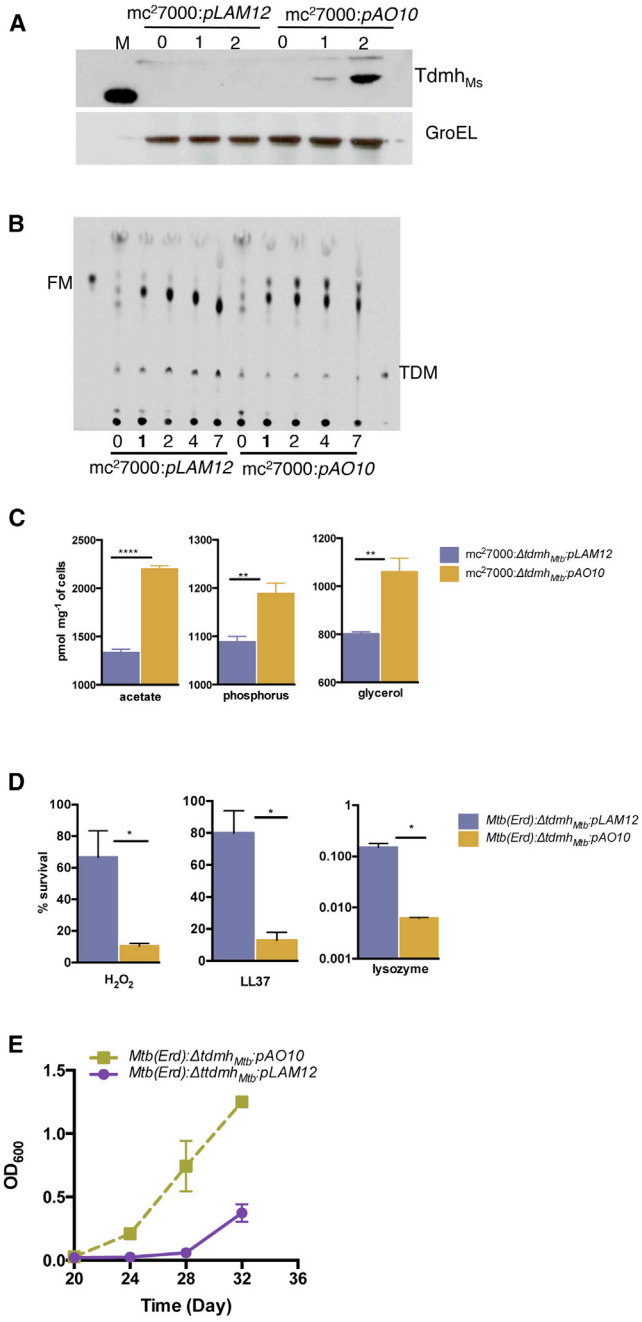

Figure 4. Ectopic Induction of TDM Hydrolase Increases Nonselective Permeability of the Mtb Envelope

(A and B) Shown are western blot (A) and lipid analysis (B) of acetamide-induced expression of $tdmh_{Ms}$ in mc²7000:*pAO10* and the empty plasmid control, mc²7000:*pLAM12*, in Sauton's media for the time (day) indicated on each lane. Purified TDM and FMs were markers on TLC in (B).

(C) Accumulation of glycerol, phosphorus, and acetate over 2 hr by acetamide-induced expression of $tdmh_{Ms}$ in mc²7000:$\Delta tdmh_{Mtb}$:*pAO10* and the empty plasmid control, mc²7000:*pLAM12*, in Sauton's media.

(D) Sensitivity of the two Mtb strains described in (E) to H_2O_2 (40 mM), lysozyme (6 μg/ml), and LL37 (20 μM).

(E) Growth of Mtb (Erd):$\Delta tdmh_{Mtb}$:*pAO10* and Mtb(Erd):$\Delta tdmh_{Mtb}$:*pLAM12* in media with limiting glycerol (0.1% v/v) and inducer (0.2% v/v acetamide).

Data in (C), (D), and (E) represent mean ± SE (n = 3). *p < 0.05, **p < 0.01, ****p < 0.0001 (t test).

lifespans than those infected with the wild-type strain (Figure S4G). It is notable that levels of phthiocerol dimycoserosate (PDIM) were the same in wild-type and $\Delta tdmh_{Mtb}$ (Figure S4H), therefore confirming that the relative increase in virulence of $\Delta tdmh_{Mtb}$ was not an artifact of a spontaneous loss of PDIM, as reported to often occur in H37Rv (Domenech and Reed, 2009).

It is notable that a constitutive expression of $tdmh_{Ms}$ from the *hsp60* promoter (pYY1) in intracellular $\Delta tdmh_{Mtb}$ also led to both a significant increase in ^{14}C incorporation from the extracellular media as well as an increased sensitivity to extracellular isoniazid (Figures 5E and 5F). Moreover, infection of C57BL/6 with $\Delta tdmh_{Mtb}$:*pYY1* during the first 3 weeks produced a burden 3-fold lesser than that of the empty plasmid strain, $\Delta tdmh_{Mtb}$:*pJL37* (Figure 5G). Taken together, complementation by $tdmh_{Ms}$ affirms that intracellular behavior of $\Delta tdmh_{Mtb}$ is directly linked to the loss of TDM hydrolase activity in the mutant. Moreover, the enzyme clearly has an important role in self-restricting intracellular growth of Mtb in an immunocompetent host through mechanisms that include stress sensitization of bacteria.

TDM Hydrolases Provide Growth Advantage to Intracellular Mtb in MyD88$^{-/-}$ Hosts

We next argued that reduced levels of intracellular stress in an immunocompromised host could mitigate the effects of TDM hydrolase-dependent stress sensitization, such that the hydrolase-dependent nutrient influx could then produce a net positive growth of Mtb in such a host. Indeed, growth of Mtb(Erd):$\Delta tdmh_{Mtb}$ in preactivated primary MyD88$^{-/-}$ BMMs was significantly slower than that in wild-type Mtb(Erd), and the complement strain (Figures 6A and S5A). MyD88 is a central adaptor molecule that converges multiple Toll-like receptor (TLR)-dependent signals to activate a strong innate antimicrobial activity against bacterial infection, including TB, in mice (Hawn et al., 2006; Scanga et al., 2004). We further observed a retarded incorporation of the radiolabel in the intracellular $\Delta tdmh_{Mtb}$ when ^{14}C-labeled acetate was added to the medium of infected primary MyD88$^{-/-}$ BMMs (Figure 6B), suggesting that slower growth of the mutant in MyD88$^{-/-}$ BMMs is likely due to slower influx of nutrients in bacteria. Importantly, constitutive expression of $Tdmh_{Ms}$ in $\Delta tdmh_{Mtb}$ produced opposing effects on its growth in preactivated primary BMMs from C57BL/6 and MyD88$^{-/-}$ mice (Figures 6C, 6D, S5B, and S5C). Finally, the slower growth characteristic of $\Delta tdmh_{Mtb}$ in MyD88$^{-/-}$ BMMs was faithfully reproduced in the lungs of the immunocompromised mice (Figure 6E), with prolonged survival of the animals (Figure 6F). Taken together, the overall effect of Tdmh on intracellular growth of Mtb during the early phase of infection is highly responsive to the innate resistance from the host.

DISCUSSION

In this study, we have discovered an adaptative response in Mtb under nutrient limitation. The response involves a hydrolase-dependent increase in nonselective permeability of the envelope and subsequent enhancement in nutrient influx through cleavage of the ester linkage of TDM. This is likely a conserved mechanism in environmental and pathogenic mycobacteria, suggested not only by the presence of $tdmh_{Mtb}$ homologs in

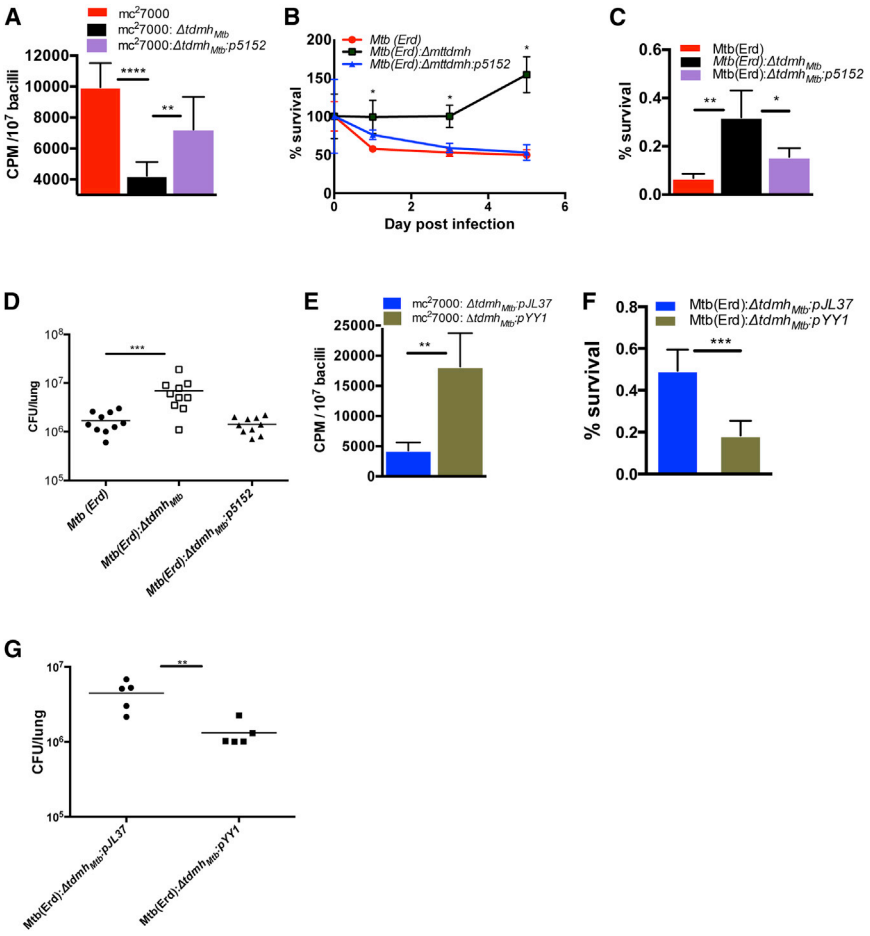

Figure 5. The Opposing Effects of $Tdmh_{Mtb}$ Self-Restrict Intracellular Growth of Mtb in the Immunocompetent Host

(A) Accumulation of radioactivity over a 48 hr period in the intracellular mc²7000, mc²7000: *Δtdmh*$_{Mtb}$, and mc²7000: *Δtdmh*$_{Mtb}$*:p5152* when ^{14}C-labeled acetate was added to the medium of infected RAW264.7 (mean ± SE; n = 7).

(B) Survival of Mtb (Erd), Mtb (Erd):*Δtdmh*$_{Mtb}$, and Mtb (Erd):*Δtdmh*$_{Mtb}$*:p5152* in activated BMMs from C57BL/6 mice (see also Figure S4C for raw cfu).

(C) Sensitivity of intracellular Mtb (Erd), Mtb (Erd):*Δtdmh*$_{Mtb}$, and Mtb (Erd):*Δtdmh*$_{Mtb}$*:p5152* to 5-day exposure of isoniazid (0.75 μg/ml) added to the culture medium of infected primary BMMs (C57BL/6) (mean ± SE; n = 5).

(D) Burden of the three Mtb strains in the lungs of C57BL/6 mice 3 weeks after aerosolized infection with ~50–100 bacilli/lung. Data represent two independent exposures, each with five animals/per strain ($p < 0.0001$, Mann-Whitney test).

(E) Relative change in intracellular accumulation of radioactivity over a 48 hr period between mc²7000: *Δtdmh*$_{Mtb}$ constitutively expressing *tdmh*$_{Ms}$ (mc²7000:*Δtdmh*$_{Mtb}$*: pYY1*) and its corresponding empty vector control, mc²7000: *Δtdmh*$_{Mtb}$*:pJL37*, when ^{14}C-labeled acetate was added to the medium of infected RAW264.7 (mean ± SE; n = 4).

(F) Sensitivity of intracellular Mtb(Erd):*Δtdmh*$_{Mtb}$*:pYY1* and Mtb(Erd):*Δtdmh*$_{Mtb}$*:pJL37* to 5-day exposure of isoniazid (0.75 μg/ml), added to the culture medium of infected primary BMMs from C57BL/6 mice (mean ± SE; n = 6).

(G) Burden of Mtb(Erd):*Δtdmh*$_{Mtb}$*:pYY1* and Mtb(Erd):*Δtdmh*$_{Mtb}$*:pJL37* in the lungs of C57BL/6 mice after 3 weeks of infection ($p < 0.01$, Mann-Whitney test). See also Figure S4.

In (A), (C), (E), and (F), *$p < 0.05$, **$p < 0.01$, ***$p < 0.001$, ****$p < 0.0001$ (t test).

several mycobacterial species, but also by the functional complementarity between $Tdmh_{Ms}$ and $Tdmh_{Mtb}$.

$Tdmh_{Mtb}$ and $Tdmh_{Ms}$ are members of a ubiquitous serine hydrolase superfamily, representing enzymes with a wide range of function, such as carboxypeptidases, proteases, phospholipases, fungal cutinases, and phage lysins (Akoh et al., 2004; Ollis et al., 1992; Payne et al., 2009), but only a few of these have been implicated in nutrient influx during bacterial adaptation. One such serine hydrolase, a deacylase of lipid A (*pagL*), in *Pseudomonas aeruginosa* is functionally comparable to $Tdmh_{Mtb}$. PagL induces outer membrane remodeling under in vitro growth in limiting magnesium conditions (Ernst et al., 2006). Loss of PagL activity is also associated with severe pulmonary infection (Ernst et al., 2006).

Implication of TDM hydrolase in mycobacterial adaptation to limiting nutrients is of particular significance in the context of resuscitation-promoting factors (Rpf), which have been widely explored for their role in mycobacterial growth after dormancy (Mukamolova et al., 1998). Mtb genome encodes five *rpf* homologs, *rpfA–rpfE*, of which *rpfB*, *rpfD*, and *rpfE* deletion impairs growth revival from late stationary phase, and *ΔrpfB* is retarded in reactivating TB in mice (Downing et al., 2005; Tufariello et al., 2006). Moreover, RpfB has a lysozyme-like structure and interacts with a peptidoglycan hydrolase, RipA (Cohen-Gonsaud et al., 2005; Hett et al., 2010), suggesting that Rpf-dependent resuscitation of Mtb also involves a limited digestion of the envelope. However, Rpf-dependent resuscitation and $Tdmh_{Mtb}$-dependent adaptation appear to represent distinct physiological states of Mtb. Whereas Rpf-dependent envelope remodeling is likely a specialized process exclusively associated with growth revival from dormancy, activity of $Tdmh_{Mtb}$ might occur over a dynamic range in metabolically active Mtb to facilitate its rapid adaptation and growth maintenance under conditions of limiting nutrients. While enhanced influx of small hydrophilic nutrients through induced envelope permeability is clearly the key Tdmh-dependent adaptative mechanism, $Tdmh_{Mtb}$ can also be argued to facilitate recycling of trehalose and mycolic acids in Mtb. However, $Tdmh_{Mtb}$-dependent nutrient recycling is likely to be secondary to other recycling mechanisms since trehalose recycling is critical for the survival of intracellular Mtb (Kalscheuer et al., 2010).

The regulated increase of nonselective nutrient influx through TDM hydrolysis provides a unique perspective of the structural, as well as functional, plasticity of the mycobacterial envelope, the permeability of which is restricted by the inner plasma

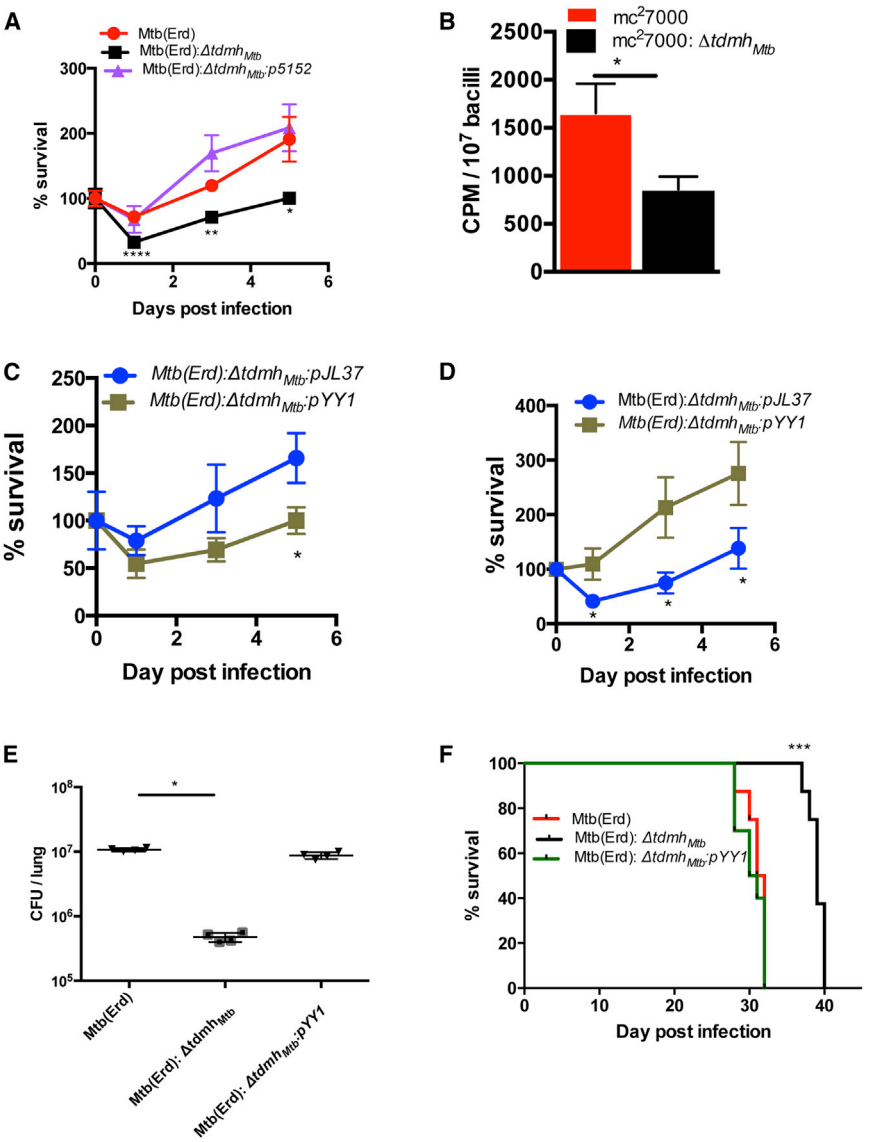

Figure 6. Tdmh Facilitates Mtb Growth in MyD88$^{-/-}$ Mice

(A) Growth of Mtb (Erd) or Mtb (Erd):*Δtdmh*$_{Mtb}$ and the complement *Δtdmh*$_{Mtb}$:p5152 strains in activated primary BMMs from MyD88$^{-/-}$ mice.

(B) Accumulation of radioactivity over a 48 hr period in the intracellular mc^{2}7000 and mc^{2}7000: *Δtdmh*$_{Mtb}$ when ^{14}C-labeled acetate was added to the medium of infected primary BMMs from MyD88$^{-/-}$ mice.

(C and D) Relative difference between the survival of Mtb (Erd):*Δtdmh*$_{Mtb}$ expressing *tdmh*$_{Ms}$ (Mtb(Erd): *Δtdmh*$_{Mtb}$:*pYY1*) and its corresponding empty vector control, Mtb (Erd):*Δtdmh*$_{Mtb}$:*pJL37*, in primary BMMs from C57BL/6 (C) and MyD88$^{-/-}$ (D) mice. Data in (A)–(D) represent mean ± SE (n = 3). *p < 0.05, **p < 0.01, ****p < 0.0001 (t test).

(E) Burden of Mtb(Erd), Mtb(Erd):*Δtdmh*$_{Mtb}$, and Mtb(Erd):*Δtdmh*$_{Mtb}$:*pYY1* in the lungs of MyD88$^{-/-}$ mice after 14 days of aerosolized infection (n = 5; p < 0.05, Mann-Whitney test). Mean burdens of the 3 strains after 24 hr of exposure were 93, 89, and 99, respectively.

(F) Survival of MyD88$^{-/-}$ mice infected with each of the three strains described in (E) (n = 8; p < 0.001, Mann-Whitney test). Raw cfu data for (A), (C), and (D) are provided in Figures S5A, S5B, and S5C, respectively. See also Figure S5.

membrane and the outer MoM (Niederweis, 2008). Permeability across MoM appears to be primarily nonselective, facilitated by the activity of channel proteins (Niederweis, 2008). It is therefore reasonable to argue that TDM hydrolases could modulate the solute influx through changes in MoM structure, implying that TDM is likely localized in MoM. This notion is further supported by the accessibility of TDM to exogenous Tdmh$_{Ms}$ (Yang et al., 2013). An increase in MoM permeability through hydrolase activity can be imagined to occur through either delocalized increase in fluidity of the lipid bilayer or localized perturbation of the lipid domains around porins to induce channel openings. However, esterase-dependent stress sensitization might be a combined effect of increased influx of the small hydrophilic solutes, such as isoniazid and peroxide, as well as greater exposure of the cell envelope targets to the external hazards. The later mechanism likely provides an explanation for the Tdmh-dependent sensitization to lysozyme and antimicrobial peptides.

Tdmh$_{Mtb}$-dependent increase in nutrient influx during the early phase of infection is not surprising given that Mtb must actively replicate in a nutrient-deprived intracellular environment in order to establish a successful infection. However, the positive effect of Tdmh on Mtb growth is clearly outweighed by the negative effects from increased sensitization of the pathogen to the intracellular stresses, as well as greater induction of inflammatory response in macrophages. Together, these opposing effects of Tdmh appear to balance the overall intracellular bacterial growth in immunocompetent hosts (Figure 7). The development of severe disease by *Δtdmh*$_{Mtb}$ raises a possibility that restricted bacterial growth during the early phase could be crucial for controlled disease progression during the chronic phase. Further immunological characterization of the host will offer crucial mechanistic insight into Tdmh-dependent disease progression. The retarded growth of *Δtdmh*$_{Mtb}$ in the MyD88$^{-/-}$ host can be reasonably linked to the physiological deficiency of the mutant in assimilating adequate nutrients. Therefore, hydrolase-dependent nutrient influx could also lead to accelerated growth of Mtb and faster reactivation of infection in other unrelated immunocompromised host conditions, including animal models described for reactivation of TB latency (Scanga et al., 1999). Analysis of *Δtdmh*$_{Mtb}$ growth and pathogenesis in such models will likely offer insight into reactivation of latent TB.

In summary, distinct consequences of TDM hydrolases on Mtb infection in immunocompetent and immunocompromised

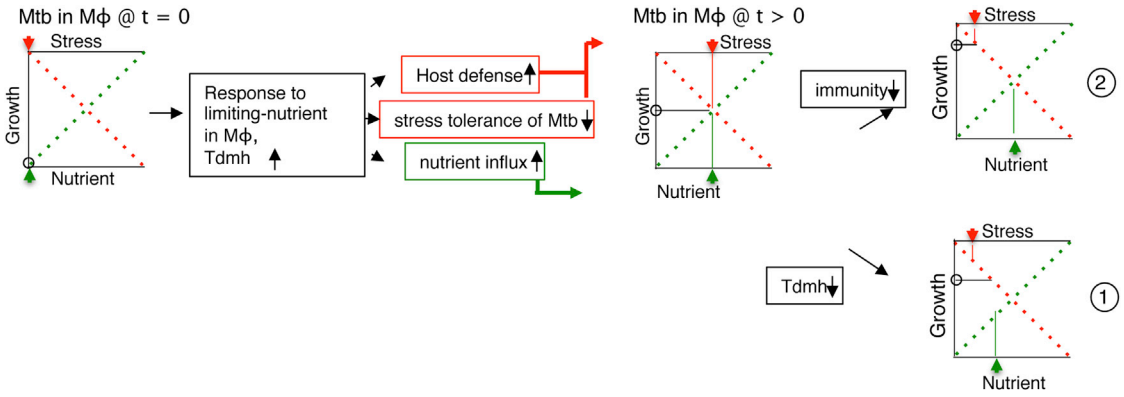

Figure 7. Schematic Representation of $Tdmh_{Mtb}$-Dependent Self-Balanced Growth of Intracellular Mtb in the Immunocompetent Host

The status of nutrient availability, stress effect, and net growth of Mtb in Mϕ at initial (t = 0) and later (t > 0) phases of infection are represented by a green arrow, red arrow, and open circle, respectively. Two possible scenarios under which this balance could be perturbed are depicted. Scenario 1 shows the effect of $Tdmh_{Mtb}$ inactivation on bacterial burden in the immunocompetent host. Although the nutrient influx in a $\Delta tdmh_{Mtb}$ mutant is likely retarded, this deficiency is outweighed by increased tolerance of the mutant to the host-induced stresses. In scenario 2, reduced intracellular stress in an immunocompromised host can mitigate the effect of $Tdmh_{Mtb}$ on stress sensitivity such that Tdmh-dependent nutrient assimilation can accelerate the growth of wild-type Mtb in such a host.

hosts not only reveal the complexities of host-pathogen dynamics, but also underscore the significance of developing distinct strategies for TB treatment depending on the status of the host immunity.

EXPERIMENTAL PROCEDURES

Bacterial Strains and Media

Except for the growth conditions described for an individual experiment in the Results, strains of Mtb, *M. smegmatis*, and *E. coli* were routinely maintained under standard conditions. Detailed growth conditions for these strains are provided in the Supplemental Information.

Construction of Mutants and Plasmids

Construction of mc^2155:$\Delta tdmh_{Ms}$ is described previously (Ojha et al., 2010). Deletion of $tdmh_{Ms}$ in various strains of Mtb was constructed using the gene replacement technique described earlier (Bardarov et al., 2002). Detailed methods for construction of these mutants and other recombinant strains are provided in the Supplemental Information. Lists of all plasmids, bacterial strains, and oligonucleotides used in this study are provided in Tables S1, S2, and S3.

Real-Time PCR

Real-time PCR was performed on a StepOnePlus RT-PCR System (Applied Biosystems) with SYBR Green Master Mix following the manufacturer's instructions. Total RNA from the desired bacterial cultures was extracted using RiboPure Kit (Ambion) and processed for real-time PCR as described in the Supplemental Information.

In Vitro Activity of TDMH

^{14}C-labeled TDM equivalent to 100,000 cpm was homogeneously suspended in the assay buffer as described earlier. The homogenate was then mixed with either 5 μg of purified $Tdmh_{Ms}$ (MSMEG_1529) or 100 μg lysates of mc^2155: $\Delta tdmh_{Ms}$: pJL37, mc^2155: $\Delta tdmh_{Ms}$: pRv3451, or mc^2155: $\Delta tdmh_{Ms}$: pRv3452 and incubated at 37°C for 2 hr. The lipids present in the reaction mixture were then extracted and analyzed as described previously (Ojha et al., 2010).

Lipid Purification and Analysis

Acetic acid, sodium salt [1-^{14}C] (1 μCi/ml; PerkinElmer) was added to either biofilms or planktonic cultures of Mtb as described in the text and incubated for either 6 (for biofilms) or 3 (for planktonic) hr before proceeding to the lipid extraction. Apolar and polar lipids were extracted and analyzed as described earlier (Ojha et al., 2010). Further details are described in the Supplemental Information.

Infection of Macrophages

For primary macrophages, bone marrow from femurs of 60-day-old female C57BL/6 and in-house-bred $MyD88^{-/-}$ mice (Hawn et al., 2006) were flushed and incubated in Dulbecco's modified Eagle's medium (DMEM) with 0.58 g/l of L-glutamine and 1 mM sodium pyruvate (Corning Life Sciences), 20% v/v fetal bovine serum (FBS; Life Technologies), and 30% v/v L929 cell-conditioned medium at 37°C for 7 days with 5% CO_2. L929 cells were cultured in DMEM with 0.58 g/l of L-glutamine, 1 mM sodium pyruvate, 10% v/v FBS, 2% v/v sodium bicarbonate (Fisher Scientific), and 1% v/v nonessential amino acids (Sigma-Aldrich) to get L929 cell supernatant. For RAW264.7 cells, L929 supernatant was substituted with 2% v/v sodium bicarbonate, and FBS was reduced to 10% v/v. Cells were seeded in 12-well plates (CELLSTAR) at 200,000 cells/well and incubated for 24 hr before infection. If necessary, BMMs were activated with 30 ng/ml of rINF-γ (Sino Biological Inc.) for 16 hr, followed by 1 μg/ml of lipopolysaccharide (LPS) (Sigma-Aldrich) for 2 hr. Desired strains of Mtb were added to the cultured cells at an moi of 10. After 6 hr, infected macrophages were washed thrice with PBS and incubated in fresh media. Cells were collected at the specified time and lysed in PBS with 0.05% SDS, and intracellular bacteria were plated on 7H11OADC and incubated for 3 weeks to determine their viability. The survival percentage of bacteria at any time was calculated with respect to mean cfu obtained at 0 days of infection. For isoniazid sensitivity of intracellular Mtb, the antibiotic was added to the cell culture media at 0.75 μg/ml after 4 hr of incubation of the washed, infected BMM in fresh media. Bacteria from the drug-exposed infected lysates were plated to determine the relative survival efficiency as compared to that of the parallel cultures of infected macrophages not exposed to antibiotics.

Nutrient Influx Assay In Vitro

Influx of radiolabeled hydrophilic solutes in various bacterial strains was determined as described previously (Stephan et al., 2005). Detailed methods are provided in the Supplemental Information.

Nutrient Uptake Assay for Intracellular Mtb

Macrophages were seeded in a 75 cm^2 flask (10^7 cells/flask) and incubated for 24 hr before infection. Desired strains of Mtb (mc^27000) were added to the cultured cells at an moi of 10. After 6 hr, infected macrophages were washed thrice with PBS and incubated in fresh media with 1 μCi/ml of acetic acid, sodium salt [1-^{14}C] (PerkinElmer) for 48 hr. Cells were washed thrice with

PBS and lysed in 1 ml of PBS with 0.05% SDS. A 10 μl aliquot from each lysate was diluted and plated to determine the total number of bacteria in the lysate. Then, a 1 ml suspension of TB-Beads (MicroSense) was added to the lysates and mixed for 5 min. After separation of TB-Beads on a magnetic plate and three washes in 1 ml PBS with 0.05% Tween 80 (PBST), the beads were suspended in 1 ml PBST. A 10 μl aliquot from each suspension was serially diluted and plated on 7H11OADC with pantothenic acids to determine the number of bacilli captured on the beads. The rest of the beads were mixed with an equal volume of 10% buffered formalin phosphate (Fisher) containing 0.1 M LiCl and collected on a 0.45 μm Spin-X Centrifuge Tube Filter (Costar). The radioactivity on the column was counted in a liquid scintillation counter (Beckman Coulter). After subtracting background counts (from the lysates of uninfected macrophages), the values across the samples were normalized to cpm/10^7 bacilli.

Mouse Infection

All mouse procedures were performed in an animal biosafety level 3 (Animal-BSL3) laboratory using the protocol approved by the Institutional Animal Care and Use Committee of the University of Pittsburgh and Seattle Biomedical Research Institute. Strains of Mtb(Erd) and its derivatives, as described, were grown to optical density 0.3 ($OD_{0.3}$), washed in PBS with Tween 80 (PBST), and resuspended to ~10^7 colony-forming units (cfu)/ml in PBST. Female C57BL/6 (Charles River Laboratories) and male MyD88$^{-/-}$ mice (Osaka University) (60 days old) were infected with aerosolized suspension of the bacterial strains for 20 min using an Inhalation Exposure System. After 24 hr of exposure, 4–5 C57BL/6 or 2 MyD88$^{-/-}$ mice from each infected group were euthanized, and bacterial burdens in the lungs were determined by homogenizing the tissues in PBST and plating the dilutions on 7H11OADC. Bacterial burdens in the organs were subsequently determined at time intervals as specified. For histopathological analysis, organs were fixed in phosphate-buffered formalin (10%) and paraffin embedded, and their ultrathin sections were stained with hematoxylin and eosin (H&E).

Statistical Analysis

Unless otherwise specified, the significance of the difference between control and experimental groups was calculated by t test (either paired or unpaired) with GraphPad Prism software. A minimum of three independent biological replicates were used. *$p < 0.05$, **$p < 0.01$, and ***$p < 0.001$.

SUPPLEMENTAL INFORMATION

Supplemental Information includes Supplemental Experimental Procedures, five figures, and three tables and can be found with this article online at http://dx.doi.org/10.1016/j.chom.2014.01.008.

ACKNOWLEDGMENTS

We thank David Sherman for the kind gift of the PDIM-deficient mutant (H37Rv:Tn2935); Beth Juneko and Dat Mai for technical help; Joanne Flynn and the Flynn laboratory for helpful discussions regarding experimental design; and Graham Hatfull, Keith Derbyshire, and Pallavi Ghosh for critical comments on the manuscript. This work was supported by NIH grants to A.K.O. (AI79288, UL1 RR024153).

Received: April 23, 2013
Revised: November 26, 2013
Accepted: January 23, 2014
Published: February 12, 2014

REFERENCES

Akoh, C.C., Lee, G.C., Liaw, Y.C., Huang, T.H., and Shaw, J.F. (2004). GDSL family of serine esterases/lipases. Prog. Lipid Res. *43*, 534–552.

Bardarov, S., Bardarov Jr, S., Jr., Pavelka Jr, M.S., Jr., Sambandamurthy, V., Larsen, M., Tufariello, J., Chan, J., Hatfull, G., and Jacobs Jr, W.R., Jr. (2002). Specialized transduction: an efficient method for generating marked and unmarked targeted gene disruptions in Mycobacterium tuberculosis, M. bovis BCG and M. smegmatis. Microbiology *148*, 3007–3017.

Belisle, J.T., Vissa, V.D., Sievert, T., Takayama, K., Brennan, P.J., and Besra, G.S. (1997). Role of the major antigen of Mycobacterium tuberculosis in cell wall biogenesis. Science *276*, 1420–1422.

Betts, J.C., Lukey, P.T., Robb, L.C., McAdam, R.A., and Duncan, K. (2002). Evaluation of a nutrient starvation model of Mycobacterium tuberculosis persistence by gene and protein expression profiling. Mol. Microbiol. *43*, 717–731.

Beutler, B. (2004). Innate immunity: an overview. Mol. Immunol. *40*, 845–859.

Brennan, P.J., and Nikaido, H. (1995). The envelope of mycobacteria. Annu. Rev. Biochem. *64*, 29–63.

Brust, B., Lecoufle, M., Tuaillon, E., Dedieu, L., Canaan, S., Valverde, V., and Kremer, L. (2011). Mycobacterium tuberculosis lipolytic enzymes as potential biomarkers for the diagnosis of active tuberculosis. PLoS ONE *6*, e25078.

Chan, J., and Flynn, J. (2004). The immunological aspects of latency in tuberculosis. Clin. Immunol. *110*, 2–12.

Cohen-Gonsaud, M., Barthe, P., Bagnéris, C., Henderson, B., Ward, J., Roumestand, C., and Keep, N.H. (2005). The structure of a resuscitation-promoting factor domain from Mycobacterium tuberculosis shows homology to lysozymes. Nat. Struct. Mol. Biol. *12*, 270–273.

Cooper, A.M., Mayer-Barber, K.D., and Sher, A. (2011). Role of innate cytokines in mycobacterial infection. Mucosal Immunol. *4*, 252–260.

Domenech, P., and Reed, M.B. (2009). Rapid and spontaneous loss of phthiocerol dimycocerosate (PDIM) from Mycobacterium tuberculosis grown in vitro: implications for virulence studies. Microbiology *155*, 3532–3543.

Downing, K.J., Mischenko, V.V., Shleeva, M.O., Young, D.I., Young, M., Kaprelyants, A.S., Apt, A.S., and Mizrahi, V. (2005). Mutants of Mycobacterium tuberculosis lacking three of the five rpf-like genes are defective for growth in vivo and for resuscitation in vitro. Infect. Immun. *73*, 3038–3043.

Ernst, J.D. (2012). The immunological life cycle of tuberculosis. Nat. Rev. Immunol. *12*, 581–591.

Ernst, R.K., Adams, K.N., Moskowitz, S.M., Kraig, G.M., Kawasaki, K., Stead, C.M., Trent, M.S., and Miller, S.I. (2006). The Pseudomonas aeruginosa lipid A deacylase: selection for expression and loss within the cystic fibrosis airway. J. Bacteriol. *188*, 191–201.

Fabrino, D.L., Bleck, C.K., Anes, E., Hasilik, A., Melo, R.C., Niederweis, M., Griffiths, G., and Gutierrez, M.G. (2009). Porins facilitate nitric oxide-mediated killing of mycobacteria. Microbes Infect. *11*, 868–875.

Ford, C.B., Lin, P.L., Chase, M.R., Shah, R.R., Iartchouk, O., Galagan, J., Mohaideen, N., Ioerger, T.R., Sacchettini, J.C., Lipsitch, M., et al. (2011). Use of whole genome sequencing to estimate the mutation rate of Mycobacterium tuberculosis during latent infection. Nat. Genet. *43*, 482–486.

Gill, W.P., Harik, N.S., Whiddon, M.R., Liao, R.P., Mittler, J.E., and Sherman, D.R. (2009). A replication clock for Mycobacterium tuberculosis. Nat. Med. *15*, 211–214.

Hawn, T.R., Smith, K.D., Aderem, A., and Skerrett, S.J. (2006). Myeloid differentiation primary response gene (88)- and toll-like receptor 2-deficient mice are susceptible to infection with aerosolized Legionella pneumophila. J. Infect. Dis. *193*, 1693–1702.

Hett, E.C., Chao, M.C., and Rubin, E.J. (2010). Interaction and modulation of two antagonistic cell wall enzymes of mycobacteria. PLoS Pathog. *6*, e1001020.

Hoffmann, C., Leis, A., Niederweis, M., Plitzko, J.M., and Engelhardt, H. (2008). Disclosure of the mycobacterial outer membrane: cryo-electron tomography and vitreous sections reveal the lipid bilayer structure. Proc. Natl. Acad. Sci. USA *105*, 3963–3967.

Hunter, R.L., Olsen, M.R., Jagannath, C., and Actor, J.K. (2006). Multiple roles of cord factor in the pathogenesis of primary, secondary, and cavitary tuberculosis, including a revised description of the pathology of secondary disease. Ann. Clin. Lab. Sci. *36*, 371–386.

Ishikawa, E., Ishikawa, T., Morita, Y.S., Toyonaga, K., Yamada, H., Takeuchi, O., Kinoshita, T., Akira, S., Yoshikai, Y., and Yamasaki, S. (2009). Direct recognition of the mycobacterial glycolipid, trehalose dimycolate, by C-type lectin Mincle. J. Exp. Med. *206*, 2879–2888.

Kalscheuer, R., Weinrick, B., Veeraraghavan, U., Besra, G.S., and Jacobs, W.R., Jr. (2010). Trehalose-recycling ABC transporter LpqY-SugA-SugB-SugC is essential for virulence of Mycobacterium tuberculosis. Proc. Natl. Acad. Sci. USA *107*, 21761–21766.

Lin, P.L., Rodgers, M., Smith, L., Bigbee, M., Myers, A., Bigbee, C., Chiosea, I., Capuano, S.V., Fuhrman, C., Klein, E., and Flynn, J.L. (2009). Quantitative comparison of active and latent tuberculosis in the cynomolgus macaque model. Infect. Immun. *77*, 4631–4642.

Mailaender, C., Reiling, N., Engelhardt, H., Bossmann, S., Ehlers, S., and Niederweis, M. (2004). The MspA porin promotes growth and increases antibiotic susceptibility of both Mycobacterium bovis BCG and Mycobacterium tuberculosis. Microbiology *150*, 853–864.

Molle, V., Saint, N., Campagna, S., Kremer, L., Lea, E., Draper, P., and Molle, G. (2006). pH-dependent pore-forming activity of OmpATb from Mycobacterium tuberculosis and characterization of the channel by peptidic dissection. Mol. Microbiol. *61*, 826–837.

Mukamolova, G.V., Kaprelyants, A.S., Young, D.I., Young, M., and Kell, D.B. (1998). A bacterial cytokine. Proc. Natl. Acad. Sci. USA *95*, 8916–8921.

Niederweis, M. (2008). Nutrient acquisition by mycobacteria. Microbiology *154*, 679–692.

Niederweis, M., Danilchanka, O., Huff, J., Hoffmann, C., and Engelhardt, H. (2010). Mycobacterial outer membranes: in search of proteins. Trends Microbiol. *18*, 109–116.

Nikaido, H. (2003). Molecular basis of bacterial outer membrane permeability revisited. Microbiol. Mol. Biol. Rev. *67*, 593–656.

Ojha, A.K., Baughn, A.D., Sambandan, D., Hsu, T., Trivelli, X., Guerardel, Y., Alahari, A., Kremer, L., Jacobs, W.R., Jr., and Hatfull, G.F. (2008). Growth of Mycobacterium tuberculosis biofilms containing free mycolic acids and harbouring drug-tolerant bacteria. Mol. Microbiol. *69*, 164–174.

Ojha, A.K., Trivelli, X., Guerardel, Y., Kremer, L., and Hatfull, G.F. (2010). Enzymatic hydrolysis of trehalose dimycolate releases free mycolic acids during mycobacterial growth in biofilms. J. Biol. Chem. *285*, 17380–17389.

Ollis, D.L., Cheah, E., Cygler, M., Dijkstra, B., Frolow, F., Franken, S.M., Harel, M., Remington, S.J., Silman, I., Schrag, J., et al. (1992). The alpha/beta hydrolase fold. Protein Eng. *5*, 197–211.

Park, I.N., Ryu, J.S., and Shim, T.S. (2008). Evaluation of therapeutic response of tuberculoma using F-18 FDG positron emission tomography. Clin. Nucl. Med. *33*, 1–3.

Payne, K., Sun, Q., Sacchettini, J., and Hatfull, G.F. (2009). Mycobacteriophage Lysin B is a novel mycolylarabinogalactan esterase. Mol. Microbiol. *73*, 367–381.

Purdy, G.E., Niederweis, M., and Russell, D.G. (2009). Decreased outer membrane permeability protects mycobacteria from killing by ubiquitin-derived peptides. Mol. Microbiol. *73*, 844–857.

Rao, V., Gao, F., Chen, B., Jacobs, W.R., Jr., and Glickman, M.S. (2006). Trans-cyclopropanation of mycolic acids on trehalose dimycolate suppresses Mycobacterium tuberculosis -induced inflammation and virulence. J. Clin. Invest. *116*, 1660–1667.

Roca, F.J., and Ramakrishnan, L. (2013). TNF dually mediates resistance and susceptibility to mycobacteria via mitochondrial reactive oxygen species. Cell *153*, 521–534.

Rohde, K.H., Veiga, D.F., Caldwell, S., Balázsi, G., and Russell, D.G. (2012). Linking the transcriptional profiles and the physiological states of Mycobacterium tuberculosis during an extended intracellular infection. PLoS Pathog. *8*, e1002769.

Scanga, C.A., Mohan, V.P., Joseph, H., Yu, K., Chan, J., and Flynn, J.L. (1999). Reactivation of latent tuberculosis: variations on the Cornell murine model. Infect. Immun. *67*, 4531–4538.

Scanga, C.A., Bafica, A., Feng, C.G., Cheever, A.W., Hieny, S., and Sher, A. (2004). MyD88-deficient mice display a profound loss in resistance to Mycobacterium tuberculosis associated with partially impaired Th1 cytokine and nitric oxide synthase 2 expression. Infect. Immun. *72*, 2400–2404.

Siroy, A., Mailaender, C., Harder, D., Koerber, S., Wolschendorf, F., Danilchanka, O., Wang, Y., Heinz, C., and Niederweis, M. (2008). Rv1698 of Mycobacterium tuberculosis represents a new class of channel-forming outer membrane proteins. J. Biol. Chem. *283*, 17827–17837.

Stallings, C.L., and Glickman, M.S. (2010). Is Mycobacterium tuberculosis stressed out? A critical assessment of the genetic evidence. Microbes Infect. *12*, 1091–1101.

Stephan, J., Bender, J., Wolschendorf, F., Hoffmann, C., Roth, E., Mailänder, C., Engelhardt, H., and Niederweis, M. (2005). The growth rate of Mycobacterium smegmatis depends on sufficient porin-mediated influx of nutrients. Mol. Microbiol. *58*, 714–730.

Takayama, K., Wang, C., and Besra, G.S. (2005). Pathway to synthesis and processing of mycolic acids in Mycobacterium tuberculosis. Clin. Microbiol. Rev. *18*, 81–101.

Tobin, D.M., Roca, F.J., Oh, S.F., McFarland, R., Vickery, T.W., Ray, J.P., Ko, D.C., Zou, Y., Bang, N.D., Chau, T.T., et al. (2012). Host genotype-specific therapies can optimize the inflammatory response to mycobacterial infections. Cell *148*, 434–446.

Tufariello, J.M., Mi, K., Xu, J., Manabe, Y.C., Kesavan, A.K., Drumm, J., Tanaka, K., Jacobs, W.R., Jr., and Chan, J. (2006). Deletion of the Mycobacterium tuberculosis resuscitation-promoting factor Rv1009 gene results in delayed reactivation from chronic tuberculosis. Infect. Immun. *74*, 2985–2995.

Ulrichs, T., Kosmiadi, G.A., Jörg, S., Pradl, L., Titukhina, M., Mishenko, V., Gushina, N., and Kaufmann, S.H. (2005). Differential organization of the local immune response in patients with active cavitary tuberculosis or with nonprogressive tuberculoma. J. Infect. Dis. *192*, 89–97.

WHO (2012). The burden of diseases caused by TB. In Global Tuberculosis Report 2012Global Tuberculosis Report 2012 (Geneva: WHO Press).

Wilson, S., Lane, A., Rosedale, R., and Stanley, C. (2010). Concentration of Mycobacterium tuberculosis from sputum using ligand-coated magnetic beads. Int. J. Tuberc. Lung Dis. *14*, 1164–1168.

Yang, C.T., Cambier, C.J., Davis, J.M., Hall, C.J., Crosier, P.S., and Ramakrishnan, L. (2012). Neutrophils exert protection in the early tuberculous granuloma by oxidative killing of mycobacteria phagocytosed from infected macrophages. Cell Host Microbe *12*, 301–312.

Yang, Y., Bhatti, A., Ke, D., Gonzalez-Juarrero, M., Lenaerts, A., Kremer, L., Guerardel, Y., Zhang, P., and Ojha, A.K. (2013). Exposure to a cutinase-like serine esterase triggers rapid lysis of multiple mycobacterial species. J. Biol. Chem. *288*, 382–392.